

THE DISTRIBUTION OF MASS FOR SPIRAL GALAXIES IN CLUSTERS AND IN THE FIELD

DUNCAN A. FORBES AND BRADLEY C. WHITMORE

Space Telescope Science Institute

Received 1988 March 11; accepted 1988 September 14

ABSTRACT

A comparison is made between the mass distributions of spiral galaxies in clusters and in the field using Burstein's mass-type methodology. Both H α emission-line rotation curves and more extended H I rotation curves are used. The fitting technique for determining mass types used by Burstein and coworkers has been replaced by an objective χ^2 method. Mass types are shown to be a function of both Hubble type and luminosity, contrary to earlier results. The present data show a difference in the distribution of mass types for spiral galaxies in the field and in clusters, in the sense that mass type I galaxies, where the inner and outer velocity gradients are similar, are generally found in the field rather than in clusters, as Burstein and coworkers previously reported. This can be understood in terms of the results of Whitmore, Forbes, and Rubin, who find that the rotation curves of galaxies in the central region of clusters are generally falling, while the outer galaxies in a cluster and field galaxies tend to have flat or rising rotation curves.

Subject headings: galaxies: clustering — galaxies: internal motions — galaxies: structure

I. INTRODUCTION

The observation of rotation curves in spiral galaxies is one of the key tools for studying the structure of galaxies, and has led to the conclusion that dark matter plays an important role. Burstein and Rubin (1985, hereafter BR) have argued that if the amount of dark matter is comparable to the amount of luminous matter at each radius, the study of the mass distribution rather than the light distribution might be a more fundamental method of studying galaxies. They comment that the standard method of determining a mass model based on the luminosity profile "is a kind of 'luminosity chauvinism,' and one must ask the question, Does Nature really work this way?" Hence, they introduce the concept of a mass curve, the integral mass distribution as a function of radius. Three basic "mass types" are defined that fit a majority of the observations. They find no correlation between mass types and other observational properties of spirals, leading them to suggest that the environment may play a dominant role in determining the mass distribution. This speculation is apparently verified by Burstein *et al.* (1986, hereafter BRFW), who report a difference in the distribution of mass types for cluster galaxies compared with field galaxies, with 33% of the field galaxies being mass type I while none of the 20 cluster galaxies studied were type I.

Kent (1986) has used a more traditional approach to interpret the same rotation curve data by constructing mass models based on the luminous distribution. He shows that the luminous matter can explain the rotation curves reasonably well for a majority of the H α rotation curves. However, as pointed out by Whitmore, Forbes, and Rubin (1988, hereafter WFR), allowing independent values of $M/L(\text{bulge})$ and $M/L(\text{disk})$ may artificially result in good fits to the observations. Several other authors have also concluded that within R_{25} , the radius at the 25 mag arcsec $^{-2}$ B isophote, the luminous mass dominates over the dark mass (e.g., Athanassoula, Bosma, and Papaioannou 1987). If this is true, then the philosophical basis for Burstein's "mass-type" analysis may not be particularly useful, at least out to R_{25} , and the traditional approach using the distribution of luminous material may be more useful.

In the present paper we reexamine the data using the same mass-type methodology as BR and BRFW, but we add more

recent observations to the sample and implement an objective reduced χ^2 method for determining the mass types. A related study (WFR) examines the rotation curves themselves and computes M/L gradients to make the comparison between cluster and field spirals.

There are two questions we attempt to answer in this paper. First, do the mass types correlate with any properties of the luminous galaxy? Second, is the distribution of mass types for spiral galaxies in clusters different from the distribution for those in the field? The objective analysis of mass types is discussed in § II. In § III we discuss various correlations with luminous properties of a galaxy and with its position in a cluster. The results are summarized in § IV.

II. AN OBJECTIVE METHOD FOR DETERMINING MASS TYPES

Following the method of BR, we have constructed integral mass curves using the formula $M(R) = 2.3265 \times 10^5 V^2 R$, where M (in units of M_\odot) is the mass interior to a given radius R (in kpc), and V (in km s $^{-1}$) is the rotational velocity. This assumes a spherically symmetric potential. A Hubble constant of 50 km s $^{-1}$ Mpc $^{-1}$ is used throughout. The best fits to each of Burstein's three mass types (I, II, and III) are made using a reduced χ^2 determination.

Our program minimizes the rms scatter by shifting the mass curve in both X and Y (i.e., $\log R$ and $\log M$ parameter space) and fitting it to the templates for the three mass types defined by BR. An iterative process determines these scale factors (R_m and M_m) and the reduced χ^2 of the best fit for each curve. An observational uncertainty of ± 7.5 km s $^{-1}$, for an average rotational velocity of 150 km s $^{-1}$, is assumed for the χ^2 analysis. A value of $\chi^2 \approx 1$ indicates that the mass curve fits the template for a given mass type perfectly, with all the rms scatter being produced by the observational uncertainty. A higher value of χ^2 indicates a poorer fit. Many galaxies have $\chi^2 < 1$, indicating that we may have overestimated the intrinsic measurement uncertainty in these cases.

In most cases a single mass type can be assigned to a given mass curve because the difference in χ^2 between the best fit and the second best fit is larger than would be expected from observational measuring errors (i.e., a difference in χ^2 of more than

TABLE 1
MASS TYPES FOR THE H α -FIELD SAMPLE

Galaxy	Hubble Type	Mass Type	BR Type	Dynamic Range	I			II			III		
					R _m	M _m	χ^2	R _m	M _m	χ^2	R _m	M _m	χ^2
NGC 701 ^a	SBc	I-II	II	0.91	+0.97	+0.69	0.64	+0.69	+0.24	0.67	+0.54	+0.00	2.06
NGC 801	Sc	III	III	1.48	+0.08	-0.27	4.86	+0.40	+0.24	0.95	+0.44	+0.33	0.45
NGC 1024 ^b	Sab	II	I	1.90	-0.16	-0.39	1.27	+0.16	+0.13	0.85	+0.17	+0.18	2.24
NGC 1085	Sb	II	II	1.23	-0.61	-0.73	0.43	+0.16	+0.30	0.18	+0.24	+0.43	1.26
NGC 1087	Sc	II-III	Int	1.30	+0.27	-0.38	2.75	+0.19	-0.44	0.93	+0.14	-0.47	1.21
NGC 1325	Sbc	I	I	1.45	+0.49	+0.04	0.28	+0.40	-0.03	2.99	+0.27	-0.19	8.48
NGC 1357	Sab	I	I	1.00	-0.08	-0.28	0.57	+0.12	+0.05	2.44	+0.15	+0.11	3.25
NGC 1421	Sbc	Unc (χ^2)	Int	1.56	+0.13	-0.36	4.93	+0.18	-0.20	2.64	+0.16	-0.18	4.73
NGC 1515	Sbc	Unc (χ^2)	Unc	1.38	-0.81	-1.35	13.99	-1.37	-1.70	15.03	-0.15	-0.38	3.64
NGC 1620	Sbc	I	I	1.68	+0.36	+0.07	0.38	+0.33	+0.11	5.36	+0.24	+0.03	11.75
NGC 2590	SBb	I	Unc	0.66	-0.18	-0.49	1.73	-0.87	-0.97	2.51 ^c	-0.86	-0.81	3.92 ^c
NGC 2608	Sc	II	Unc	1.38	-1.42	-2.42	4.72 ^c	-0.53	-1.24	2.04	-0.95	-1.55	3.08
NGC 2639	Sa	III	III	0.83	+0.59	+0.78	2.94	+0.56	+0.77	0.88	+0.55	+0.77	0.23
NGC 2715	Sc	I	I	1.56	+0.41	-0.21	0.52	+0.39	-0.15	3.09	+0.27	-0.28	9.77
NGC 2742	Sc	I	I	1.30	+0.30	-0.19	0.32	+0.23	-0.23	3.81	+0.14	-0.33	7.94
NGC 2775	Sab	II-III	III	0.68	-0.40	-0.53	0.55	+0.21	+0.29	0.26	+0.25	+0.35	0.32
NGC 2815	SBb	II	II	1.60	-1.43	-1.67	1.68 ^c	-0.93	-0.86	1.09 ^c	-1.50	-1.25	2.61 ^c
NGC 2844	Sa	II	II	1.15	+0.08	-0.38	0.52	+0.06	-0.36	0.32	+0.02	-0.39	1.48
NGC 3054	Sb	III	III	1.34	+1.20	+1.37	3.21	+0.87	+0.82	4.51	+0.73	+0.66	0.54
NGC 3067	Sab	II	II	1.15	+0.37	-0.14	1.08	+0.19	-0.38	0.28	+0.12	-0.46	1.01
NGC 3145	Sbc	I	Int	1.64	-1.00	-1.31	0.54 ^c	-0.21	-0.21	1.65	-0.12	-0.03	4.02
NGC 3200	Sab	Unc (χ^2)	Unc	1.78	+0.13	+0.01	5.08	+0.21	+0.23	3.10	+0.18	+0.24	4.76
NGC 3223	Sb	Unc (χ^2)	Int	1.38	+1.20	+1.43	19.39	+0.86	+0.89	21.21	+0.75	+0.79	5.47
NGC 3281	Sa	I	Unc	0.76	-0.28	-0.68	1.85	+0.12	-0.10	3.38	+0.28	+0.10	4.00
NGC 3495	Sd	I-II	II	1.38	+0.83	+0.49	2.42	+0.66	+0.26	1.74	+0.42	-0.09	13.34
NGC 3593	Sa	II-III	III	0.62	-0.49	-1.35	1.05	-0.37	-1.15	0.11	-0.36	-1.12	0.15
NGC 3672	Sc	Unc (χ^2)	Int	1.26	+1.30	+1.35	30.68 ^d	+1.46	+1.90	22.65 ^d	+0.82	+0.62	11.70
NGC 4594	Sa	Unc (χ^2)	III	1.20	+1.10	+1.62	8.85	+0.76	+1.07	8.97	+0.66	+0.96	5.58
NGC 4605	SBc	I	I	0.78	+0.54	-0.17	0.04	+0.23	-0.67	0.12	+0.11	-0.85	1.05
NGC 4682	Sc	I	I	1.38	+0.36	-0.11	0.22	+0.29	-0.14	2.15	+0.20	-0.24	5.75
NGC 4800	Sb	I	Int	0.90	-0.68	-1.27	0.42	-0.28	-0.69	1.98	-0.26	-0.65	2.67
NGC 4845	Sab	II-III	Unc	1.15	-0.83	-1.35	4.32	-0.26	-0.55	1.89	-0.21	-0.46	2.13
NGC 6314	Sa	II-III	II	1.12	-0.93	-1.26	1.51 ^c	-0.01	-0.07	0.18	-0.10	-0.09	0.24
NGC 7083	Sbc	I	I	1.22	-0.03	-0.38	0.18	+0.41	+0.27	0.81	+0.43	+0.32	1.92
NGC 7171 ^a	SBb	III	III	0.60	+1.19	-1.35	6.40	+0.80	+0.69	7.37	+0.69	+0.57	0.88
NGC 7217	Sab	III	III	1.00	-0.80	-1.01	1.86	-0.05	-0.02	0.51	+0.01	+0.07	0.32
NGC 7537	Sbc	III	III	1.56	+0.68	+0.23	10.99	+0.46	-0.06	6.44	+0.39	-0.10	0.67
NGC 7541 ^a	SBbc	Unc (χ^2)	Unc	1.64	-1.37	-1.97	4.22 ^c	-0.51	-0.82	6.49	-1.52	-1.65	10.30 ^c
NGC 7606	Sb	III	III	0.88	+0.28	+0.12	2.43	+0.68	+0.70	0.40	+0.70	+0.74	0.24
NGC 7664	Sc	I	I	1.15	-0.08	-0.37	0.76	+0.15	+0.01	3.74	+0.18	+0.07	5.21
UGC 2885	Sc	Unc (χ^2)	I	1.48	-0.90	-1.13	3.03 ^c	-0.04	+0.04	2.41	+0.07	+0.24	4.88
UGC 3691	Sc	I	Int	1.45	+1.12	+0.71	1.75	+0.74	+0.06	3.07	+0.55	-0.19	9.05
UGC 10205	Sa	II	II	1.41	+0.80	+0.78	2.89	+0.64	+0.59	1.35	+0.47	+0.40	5.87
UGC 11810	Sb	I	I	1.38	+0.35	-0.14	0.84	+0.41	+0.02	2.81	+0.38	+0.02	5.39
UGC 12810	Sb	I	I	1.54	+0.62	+0.35	0.09	+1.00	+0.89	0.21	+1.02	+0.93	0.34
IC 467	Sc	I	I	1.68	+0.66	+0.10	0.32	+0.55	-0.01	0.71	+0.39	-0.20	6.95
IC 724 ^b	Sa	Unc(χ^2)	Int	1.00	-0.64	-0.75	11.66	+0.07	+0.23	5.90	+0.04	+0.28	2.51

50% between the two mass types; see below). In cases where this criterion is not met, two mass types are assigned (e.g., type II–III). If $\chi^2 > 2.32$ for all three fits, then the mass curve is classified as UNC (unclear). This criterion represents the 99% confidence level for 10 degrees of freedom (i.e., 12 data points for a typical galaxy in the sample minus 2 free parameters) as given in Table C-4 from Bevington (1969). The UNC designation is also used when the extent (i.e., dynamic range) of the data points is less than a factor of 3 (i.e., 0.48 in log R).

The 50% variation in χ^2 criterion used to determine whether a particular fit can be distinguished from another mass type was based on three evaluations. The first is a comparison between the mass types determined from observations taken by different observers, in this case a comparison between Chincarini and de Souza (1985) and Guhathakurta *et al.* (1988) of four galaxies. The second estimate results from fits to galaxies such as WR 42, where fairly good fits are found to types I and III, but II is worse. In many cases this is because of the kink in the mass type II curve at about -1.0 in log R . A curve which perfectly bisected the type I and type III curves would actually result in the best fit in these cases. The kink therefore introduces a certain amount of noise into the analysis. The third estimate of the uncertainty results from a subjective evaluation of when two types can be clearly differentiated. All three methods result in estimates for the uncertainty in χ^2 between 30% and 50%. We adopt the more conservative value of 50%.

A comparison was made between the original rotation curve data of Rubin *et al.* (1985) and the smoothed rotation curve advocated by BR. We conclude that the mass types do not change significantly (i.e., in only two out of 20 cases with an unambiguous mass type). Hence, in the analysis of new observations, we use the original raw data, with the caveat that in the few cases where obvious velocity variations were present (e.g., the inner region of DC 39) those particular points were excluded.

The following four samples (refer to WFR for details) were analyzed:

1. The H α -FIELD sample (47 galaxies) consists of field spirals with optical H α emission-line rotation curves as observed by Rubin *et al.* (1985).
2. The H α -CLUSTER sample (23 galaxies) comes from three sources. It consists of spiral galaxies in the Cancer, Virgo, Hercules, Pegasus I, and DC 1842–63 clusters with optical H α emission-line rotation curves as observed by Rubin *et al.* (1985), Chincarini and de Souza (1985), and Rubin, Whitmore, and Ford (1988).
3. The HI-FIELD sample (16 galaxies) comes from observations of field spirals with extended H I as compiled by Kent (1987).

4. The H I-CLUSTER sample (21 galaxies) comes from a study of Virgo Cluster spirals using the Very Large Array by Guhathakurta *et al.* (1988).

The resulting values of the scale factors (R_m and M_m), the reduced χ^2 , and the mass type for each galaxy as determined by our objective method are recorded in Tables 1 and 2 (for the H α sample) and Tables 3 and 4 (for the H I sample). When the UNC classification is given, the next symbol in the table denotes the cause (i.e., $\chi^2 > 2.32$ or DR if the dynamic range is small). We have linearly extended the original mass-type templates of BR (as given in their Table 2) in both log R and log M . Large shifts (> 1.0 in log space) above or below the original range are also recorded in these tables, as are the cases in which certain velocities are excluded, as discussed above.

Rotation curves that fit mass type I tend to have fairly similar velocity gradients at all radii, while rotation curves that fit mass type III tend to have steep inner gradients and flat outer gradients. However, it is important to note that because both the mass and the radius are allowed to shift when fitting the curves, it is not possible to characterize the three mass types as simply rising, flat, and falling rotation curves, as is often mistakenly stated in the literature. For example, in Figure 1 we show the corresponding rotation curves for two fictitious galaxies fitted to different regions of the mass type III curve. Figures 1b and 1c show that a rotation curve which is rising rapidly at all radii (when the fit is to the left-hand side of Fig. 1a), or a rotation curve that turns over and is falling (when the fit is to the right-hand side of Fig. 1a), can result in a mass type III distribution. While this is a contrived example designed to demonstrate the effect, it can also be seen by comparing NGC 4206 (mass type III; rising rotation curve) to NGC 7606 (mass type III; falling rotation curve).

III. RESULTS

a) Do Mass Types Correlate with Any Properties of the Luminous Galaxy?

Although BR acknowledge that mass type I galaxies include a large proportion of Sc galaxies, they go on to claim that mass types are “not directly a function of luminosity, of mass, of mass density, of Hubble type, or, by inference, of bulge-to-disk ratio.” If this is true, it suggests that the dark matter may dominate at all radii. This appears to contradict the results of Kent (1986, 1987), who claims that the rotation curves can be predicted fairly well from the luminous distribution, at least over most of their optical extent (see WFR for a discussion of why these fits may be artificially enhanced by Kent’s method).

With this apparent contradiction in mind, we have examined the results from Table 1 to determine whether any correlations

NOTES TO TABLE 1

- Col. (1).—NGC = *New General Catalogue* number of galaxy; UGC = *Uppsala General Catalogue* number (Nilson 1973); IC = *Index Catalog* number.
 Col. (2).—Hubble type = revised Hubble type from RC2 (de Vaucouleurs, de Vaucouleurs, and Corwin 1976), RSA (Sandage and Tammann 1981), or UGC (Nilson 1973).
 Col. (3).—Mass type = I, II, III, UNC if $\chi^2 > 2.32$ or dynamic range (DR) < 0.48 in log R space from our analysis.
 Col. (4).—BR type = mass type as determined by BR; I, II, III, UNC, or INT (having properties of more than one type).
 Col. (5).—Dynamic range = the range in log R space.
 Cols. (6), (9), and (12).— R_m = radius scale factor for our fits as defined in BR.
 Cols. (7), (10), and (13).— M_m = mass scale factor for our fits as defined in BR.
 Cols. (8), (11), and (14).— χ^2 = reduced χ^2 .
^a Inner points with large velocity changes removed.
^b Outer points with large velocity changes removed.
^c Above the original range of BR by more than 1.0 in log space.
^d Below the original range of BR by more than 1.0 in log space.

TABLE 2
MASS TYPES FOR THE H α -CLUSTER SAMPLE

Galaxy	Hubble Type	Mass Type	BRFW Type	R_{Cluster} (Mpc)	Dynamic Range	I			II			III		
						R_m	M_m	χ^2	R_m	M_m	χ^2	R_m	M_m	χ^2
Cancer Cluster														
NGC 2558	Sab	II-III	II	0.99	0.94	+0.61	+0.77	2.39	+0.61	+0.82	1.07	+0.57	+0.80	1.12
UGC 4329	Sc	III	III	0.58	1.48	+1.10	+0.80	2.87	+0.72	+0.15	3.74	+0.60	-0.01	0.30
UGC 4386	Sb	Unc (χ^2)	Int	1.29	1.56	+1.40	+1.60	9.67 ^d	+1.23	+1.43	9.13 ^d	+0.82	+0.70	5.80
Virgo Cluster														
NGC 4321 ^a	Sbc	Unc (χ^2)	I	1.38	1.45	-0.26	-0.76	7.36	-0.09	-0.43	17.25	-0.10	-0.40	23.65
NGC 4388	Sb	I-II	III	0.44	0.96	+1.32	+1.74	1.72 ^d	+0.94	+1.09	1.40	+0.58	+0.41	2.84
NGC 4402	Sb	Unc (χ^2)	III	0.47	0.65	+1.27	+1.02	29.40	+1.58	+2.00	6.61 ^d	+1.32	+1.75	5.22
NGC 4419	SBa	II	II	0.98	0.90	+0.35	+0.15	0.42	+0.13	-0.17	0.08	+0.06	-0.26	1.06
NGC 4569	Sab	II-III	III	0.58	1.28	+1.54	+1.96	12.26 ^d	+1.67	+2.53	1.84 ^d	+0.97	+1.04	1.41
NGC 4698	Sab	I	I	2.03	1.21	+0.63	+0.59	2.14	+0.39	+0.23	3.38	+0.27	+0.08	3.82
Hercules Cluster														
NGC 6045	Scd	III	III	0.25	1.16	+0.93	+1.09	10.22	+0.77	+0.89	4.28	+0.74	+0.88	2.13
NGC 6054	SBc	II-III	II	0.25	1.71	-0.82	-1.53	1.86 ^c	-0.27	-0.70	0.60	-0.21	-0.56	0.82
Peg I Cluster														
NGC 7591 ^a	SBb	Unc (χ^2)	Int	2.43	1.83	-1.63	-2.13	19.18 ^c	-0.68	-0.84	8.01 ^c	-0.65	-0.71	2.48
NGC 7608	Sb	Unc (χ^2)	III	0.56	1.30	+1.47	+1.44	13.75 ^d	+1.44	+1.65	6.48 ^d	+0.84	+0.42	7.57
NGC 7631	Sb	Unc (χ^2)	II	0.30	1.71	+0.30	-0.13	4.23	+0.50	+0.24	12.39	+0.28	-0.02	25.95
UGC 12417	Sc	I	II	4.35	1.45	+0.89	+0.47	0.57	+0.69	+0.18	0.89	+0.45	-0.17	9.37
UGC 12498 ^a	Sb	III	III	0.49	1.08	+0.95	+0.60	1.31	+0.65	+0.13	0.77	+0.55	+0.00	0.49
DC1842-63 Cluster														
DC 02	Sb	Unc (χ^2)	Int	0.68	1.21	+0.10	-0.50	7.28	+0.10	-0.44	16.18	-0.02	-0.56	22.11
DC 08 ^b	Sa	Unc (χ^2)	Int	0.24	1.30	-0.29	-0.67	4.58	-0.16	-0.45	9.05	-0.21	-0.50	10.24
DC 10 ^b	Sc(pec)	I-II	Unc	0.17	0.60	+0.80	+0.10	1.48	+0.58	-0.24	2.07	+0.42	-0.52	3.09
DC 24	SBc	III	III	0.23	1.21	+0.90	+0.42	3.39	+0.57	-0.12	3.43	+0.45	-0.31	1.30
DC 39 ^a	SBc	Unc (χ^2)	III	0.28	0.86	+0.30	-0.77	5.44	+0.58	-0.35	5.36	+0.60	-0.31	5.90
WR 42	Sa	I-III	III	1.33	1.08	+1.14	+1.27	0.71	+0.87	+0.83	1.13	+0.62	+0.48	0.62
WR 66	SBb	II	III	1.52	1.16	+0.64	+0.30	2.39	+0.62	+0.33	0.74	+0.58	+0.30	1.46

Col. (1).—NGC = *New General Catalogue* number of galaxy; UGC = *Uppsala General Catalogue* number (Nilson 1973); IC = *Index Catalogue* number.

Col. (2).—Hubble type = revised Hubble type from RC2, RSA, or UGC.

Col. (3).—Mass type = I, II, III, or UNC if $\chi^2 > 2.32$ or dynamic range (DR) < 0.48 in log R space from our analysis.

Col. (4).—BRFW type = mass type as determined by BRFW.

Col. (5).— R_{Cluster} = distance in Mpc from the cluster center. The cluster centers are assumed to be Cancer—NGC 2563; Virgo—M87; Hercules—halfway between NGC 6045 and NGC 6054; Pegasus I—halfway between NGC 7619 and NGC 7626; DC 1842–63—DC 19.

Col. (6).—Dynamic range = the range in log R space.

Cols. (7), (10), and (13).— R_m = radius scale factor for our fits as defined in BR.

Cols. (8), (11), and (14).— M_m = mass scale factor for our fits as defined in BR.

Cols. (9), (12), and (15).— χ^2 = reduced χ^2 .

^a Inner points with large velocity changes removed.

^b Outer points with large velocity changes removed.

^c Above the original range of BR by more than 1.0 in log space.

^d Below the original range of BR by more than 1.0 in log space.

exist between mass types and any other properties of the luminous galaxy. The results are displayed in Table 5. We find that mass types correlate with Hubble type (with a correlation coefficient $R = 0.47$) and B -magnitude ($R = 0.22$). The correlation between mass type and Hubble type is shown in Figure 2. It can be seen that Sa galaxies tend to be mass type II–III and Sc galaxies tend to be mass type I. We also give the correlation coefficients, in Table 5, between mass type and $B-H$ ($R = 0.29$), the outer gradient of the rotation curve (OG; $R = 0.49$), the inner gradient (IG; $R = 0.33$), and the difference between IG and OG (IG – OG; $R = 0.45$). The latter is a measure of the curvature of the mass distribution curve. The

outer gradient is defined as the percentage increase of the rotation curve between $0.4R_{25}$ and $0.8R_{25}$ normalized to the maximum rotational velocity (Whitmore 1984). The inner gradient is the percentage of the maximum rotational velocity reached by $0.15R_{25}$. One would expect various measures of the rotation curve gradient to correlate with mass type, since they are derived from the same data; we find that the OG is best.

We also carried out a mass-type analysis on Rubin's synthetic rotation curves (Rubin *et al.* 1985). These synthetic curves are essentially averages of observed rotation curves for field galaxies as a function of Hubble type and absolute B -magnitude. The scale factors (R_m and M_m), reduced χ^2 , and

TABLE 3
MASS TYPES FOR THE H I-FIELD SAMPLE

Galaxy	Hubble Type	Mass Type	Dynamic Range	I			II			III		
				R_m	M_m	χ^2	R_m	M_m	χ^2	R_m	M_m	χ^2
NGC 224	Sb	II-III	0.70	-0.30	-0.61	1.30	-0.42	-0.47	0.64	-0.51	-0.41	0.53
NGC 247	Sd	Unc (χ^2)	1.33	+0.91	+0.26	14.76	+1.05	+0.66	12.71	+0.51	-0.35	10.07
NGC 300	Sd	II	1.53	+0.82	+0.05	2.99 ^d	+0.51	-0.43	1.27	+0.33	-0.66	2.70
NGC 2403	Scd	I	1.81	+0.16	-0.59	0.56	+0.29	-0.30	3.70	+0.18	-0.39	13.00
NGC 2841	Sb	II-III	1.19	-0.67	-0.88	1.89 ^c	+0.26	+0.35	0.54	+0.28	+0.44	0.99
NGC 2903	Sbc	II-III	1.01	-0.66	-1.16	2.15	+0.16	-0.07	0.53	+0.25	+0.07	0.43
NGC 3031	Sab	Unc (χ^2)	0.86	-0.65	-1.14	12.00	+0.17	-0.05	7.11	+0.11	-0.04	3.70
NGC 3109	SBm	I-II	0.74	+0.78	-0.49	0.49	+0.61	-0.73	0.72	+0.57	-0.77	1.62
NGC 3198	SBc	II	1.64	+1.60	+0.98	3.51	+1.77	+1.31	0.14	+1.73	+1.31	0.96
NGC 4236	SBdm	III	1.07	+1.18	+0.56	3.86	+0.80	-0.08	5.29	+0.67	-0.26	0.61
NGC 4258	Sbc	I	1.08	-0.68	-1.21	1.37 ^c	-1.24	-1.49	2.19 ^c	+0.37	+0.18	4.54
NGC 4736	Sab	Unc (χ^2)	1.33	-1.48	-2.11	8.31 ^c	-0.73	-1.06	3.67	-1.21	-1.39	2.41 ^c
NGC 5033	Sc	III	1.56	-1.17	-1.65	4.89 ^c	-1.16	-1.31	1.68 ^c	-0.06	-0.12	0.95
NGC 5055	Sbc	III	1.65	-0.96	-1.53	4.74 ^c	-0.13	-0.37	1.95	+0.05	-0.08	0.66
NGC 7331	Sbc	I	0.70	+0.01	-0.29	0.57	-0.09	-0.17	1.20	-0.44	-0.37	2.12
UGC 2259	SBdm	I	0.90	+0.14	-0.89	0.37	+0.19	-0.77	0.59	+0.18	-0.76	1.08

Col. (1).—NGC = *New General Catalogue* number of galaxy; UGC = *Uppsala General Catalogue* number (Nilson 1973); IC = *Index Catalog* number.

Col. (2).—Hubble type = revised Hubble type from RC2, RSA, or UGC.

Col. (3).—Mass type = I, II, III, or UNC if $\chi^2 > 2.32$ or dynamic range (DR) < 0.48 in log R space from our analysis.

Col. (4).—Dynamic range = the range in log R space.

Cols. (5), (8), and (11).— R_m = radius scale factor for our fits as defined in BR.

Cols. (6), (9), and (12).— M_m = mass scale factor for our fits as defined in BR.

Cols. (7), (10), and (13).— χ^2 = reduced χ^2 .

^a Inner points with large velocity changes removed.

^b Outer points with large velocity changes removed.

^c Above the original range of BR by more than 1.0 in log space.

^d Below the original range of BR by more than 1.0 in log space.

adopted mass type for each synthetic rotation curve are recorded in Table 6. The correlation between mass type and absolute B -magnitude is clearly evident, with mass type I being associated predominantly with bright galaxies and mass type III with faint galaxies. The correlation between mass type and Hubble type is not as obvious.

b) Are Mass Types Dependent on Galactic Environment?

BRFW, using $H\alpha$ rotation curves, derived mass-type curves for 20 cluster spirals and concluded that “while the distribution in Hubble types between the two samples is relatively similar, the distribution of mass types is significantly different. One-third (20 out of 60) field galaxies are of mass type I; none of the 20 cluster galaxies have this mass type.” With this in mind, we analyzed the $H\alpha$ and H I samples.

i) $H\alpha$ Sample

Our best fits of the BRFW sample (and a few additional galaxies) are displayed in Figure 3. The distribution of mass types is shown in Figure 4. Comparing this with Figure 3b of BRFW, we find that our objective method has not significantly changed the distribution of mass types for the field galaxies from that of BR (only one out of 24 galaxies with unambiguous mass types differs). The small number of galaxies (nine) classi-

fied as UNC is a reflection of the quality of optical data available for field galaxies.

The distribution of the cluster sample, however, has changed slightly. We find that in cases when a clear mass type can be defined, our fit differs from that of BRFW in two out of seven galaxies. In addition, we have classified nine galaxies as UNC; BRFW classify only two galaxies as UNC. However, we substantiate the BRFW finding of a deficiency of mass type I in the cluster sample, although the statistical significance is reduced. A Kolmogorov-Smirnov test indicates a 22% chance that the two distributions are taken from the same sample.

Figure 5 shows the best fit for three galaxies, illustrating some typical differences between our analysis and that of BRFW. UGC 12417 (Sc) is a member of the Pegasus I Cluster. It has been classified by BRFW as type II. Our objective method finds I ($\chi^2 = 0.57$), II ($\chi^2 = 0.89$), and III ($\chi^2 = 9.37$); we classified it as type I. The scale factors ($R_m = 0.89$, $M_m = 0.47$) shift the data points so that the lower points lie 0.40 below the original cutoff as given by BR. WR 42 (Sa) is a member of the DC 1842–63 cluster. It has been classified by BRFW as mass type III. Our objective method finds I ($\chi^2 = 0.71$), II ($\chi^2 = 1.13$), and III ($\chi^2 = 0.62$); we classified this as type I–III. However, it is important to note that χ^2 for type II would be lower (i.e., 0.57) if the kink in the mass type II template does not exist. The kink therefore introduces a certain

FORBES AND WHITMORE

 TABLE 4
 MASS TYPES FOR THE H I-CLUSTER SAMPLE

Galaxy	Hubble Type	Mass Type	R_{Cluster} (Mpc)	Dynamic Range	I			II			III		
					R_m	M_m	χ^2	R_m	M_m	χ^2	R_m	M_m	χ^2
NGC 4178 ^a	SBdm	II-III	1.71	0.58	+0.40	-0.43	0.43	+0.78	+0.10	0.14	+0.83	+0.18	0.17
NGC 4192 ^a	Sab	II-III	1.78	0.77	+1.07	+1.01	1.44	+1.06	+1.02	0.84	+1.08	+1.06	0.65
NGC 4206 ^a	Sbc	III	1.40	0.70	+1.52	+1.23	0.43	+1.16	+0.63	0.41	+1.04	+0.44	0.11
NGC 4216 ^a	Sb	III	1.36	0.53	+1.57	+2.02	0.31	+1.19	+1.38	0.17	+1.11	+1.25	0.09
NGC 4222 ^a	Sd	Unc (DR)	1.33	0.34	+1.32	+1.05	1.05	+1.23	+0.95	0.97	+1.04	+0.60	1.37
NGC 4237 ^a	Sbc	Unc (DR)	1.57	0.22	+1.16	+1.11	0.01	+0.76	+0.44	0.02	+0.72	+0.37	0.01
NGC 4254 ^a	Sc	I	1.29	0.53	+1.14	+1.15	0.54	+1.00	+0.94	0.96	+1.00	+0.95	1.29
NGC 4303 ^a	Sbc	I	2.87	0.62	-0.11	-0.80	0.11	+0.62	+0.16	0.37	+0.71	+0.27	0.40
NGC 4321 ^a	Sbc	Unc (χ^2)	1.40	0.53	-0.10	-0.36	6.57	-0.30	-0.32	5.97	+0.66	+0.64	4.56
NGC 4388	Sb	III	0.45	0.85	+1.21	+1.46	3.20	+0.83	+0.81	3.86	+0.70	+0.61	0.72
NGC 4402	Sb	I-II	0.49	1.17	+1.26	+1.19	1.30 ^d	+0.71	+0.20	1.83	+0.42	-0.25	13.99
NGC 4450 ^a	Sab	Unc (DR)	0.42	0.26	+0.74	+0.69	0.01	+0.76	+0.72	0.01	+0.80	+0.78	0.02
NGC 4501 ^a	Sb	II	0.73	0.49	+0.44	+0.42	0.14	+0.77	+0.88	0.01	+0.81	+0.94	0.05
NGC 4535 ^a	Sc	I	1.50	0.53	+1.17	+1.17	1.27	+0.96	+0.85	2.15	+0.98	+0.89	3.11
NGC 4548 ^a	SBb	II-III	0.84	0.49	+0.84	+0.58	2.17	+0.81	+0.55	1.54	+0.90	+0.68	1.29
NGC 4568 ^a	Sbc	Unc (DR)	0.70	0.26	+0.89	+0.72	0.06	+0.82	+0.61	0.08	+0.82	+0.61	0.15
NGC 4569 ^a	Sab	II	0.59	0.91	+1.11	+1.32	0.59	+0.85	+0.91	0.37	+0.68	+0.64	3.41
NGC 4579	Sb	II-III	0.66	0.61	-0.69	-0.83	0.42	+0.17	+0.28	0.28	+0.26	+0.39	0.24
NGC 4647 ^a	Sc	Unc (DR)	1.19	0.15	+0.14	-0.65	1.42	-2.02	-2.65	0.47 ^c	+0.11	-0.48	0.01
NGC 4654 ^a	Scd	Unc (DR)	1.22	0.36	+1.77	+2.53	5.60	+1.39	+1.87	6.64	+1.61	+2.65	0.60
NGC 4689 ^a	Sbc	Unc (DR)	1.61	0.15	-0.04	-0.54	1.05	+0.22	-0.10	0.01	+0.18	-0.10	0.01

Col. (1).—NGC = *New General Catalogue* number of galaxy; UGC = *Uppsala General Catalogue* number (Nilson 1973); IC = *Index Catalog* number.

Col. (2).—Hubble type = revised Hubble type from RC2, RSA, or UGC.

Col. (3).—Mass type = I, II, III, or UNC if $\chi^2 > 2.32$ or dynamic range (DR) < 0.48 in log R space from our analysis.

Col. (4).— R_{Cluster} = distance in Mpc from the cluster center. The cluster centers assumed to be Cancer—NGC 2563; Virgo—M87; Hercules—halfway between NGC 6045 and NGC 6054; Pegasus I—halfway between NGC 7619 and NGC 7626; DC 1842—63—DC 19.

Col. (5).—Dynamic range = the range in log R space.

Cols. (6), (9), and (12).— R_m = radius scale factor for our fits as defined in BR.

Cols. (7), (10), and (13).— M_m = mass scale factor for our fits as defined in BR.

Cols. (8), (11), and (14).— χ^2 = reduced χ^2 .

^a Inner points with large velocity changes removed.

^b Outer points with large velocity changes removed.

^c Above the original range of BR by more than 1.0 in log space.

^d Below the original range of BR by more than 1.0 in log space.

amount of noise into the analysis, as explained in § II. The determination of mass type III, by BRFW, does not reflect how poorly the mass type is actually determined in this case. Shown in Figure 5 is the best fit to mass type III. NGC 4698 (Sa) is a member of the Virgo Cluster. It has been classified by BR as type I (in their field sample) but was not included in their cluster sample. Our objective method finds I ($\chi^2 = 2.14$), II ($\chi^2 = 3.38$), and III ($\chi^2 = 3.82$). Hence we also classified it as a

mass type I cluster galaxy, although it barely meets our $\chi^2 < 2.32$ criterion.

ii) H I Sample

We also performed the mass-type analysis on the H I-FIELD and H I-CLUSTER samples (see Tables 3 and 4); the best fits are displayed in Figure 6, and the distribution of mass types is shown in Figure 7.

 TABLE 5
 CORRELATIONS WITH MASS TYPE

Observational Parameter	Hubble Type	B	$B-H$	Outer Gradient (OG) ^a	Inner Gradient (IG) ^b	IG - OG
Correlation coefficient	0.47	0.22	0.29	0.49	0.33	0.45
Number of galaxies	49	49	42	42	34	34
Confidence levels ^c	99.9%	85.0%	90.0%	99.9%	95.0%	99.0%

^a OG is defined as the percentage increase of the rotation curve between $0.4R_{25}$ and $0.8R_{25}$ normalized to the maximum rotational velocity.

^b IG is defined as the percentage of the maximum rotational velocity reached by $0.15R_{25}$.

^c Probability that the correlation coefficient exceeds that of a random sample.

TABLE 6
MASS TYPES OF RUBIN'S SYNTHETIC ROTATION CURVES

M_B^a	HUBBLE TYPE	MASS TYPE	I			II			III		
			R_m	M_m	χ^2	R_m	M_m	χ^2	R_m	M_m	χ^2
-18	Sa	III	+0.89	+0.54	18.82	+0.53	-0.05	22.35	+0.40	-0.21	0.57
-19	Sa	III	+0.69	+0.41	13.88	+0.40	-0.03	9.70	+0.31	-0.12	0.52
-20	Sa	II	+0.36	+0.12	3.82	+0.23	-0.02	0.89	+0.16	-0.08	5.31
-21	Sa	I	-0.10	-0.29	1.03	+0.03	-0.03	3.92	-0.00	-0.03	9.24
-22	Sa	I	-0.70	-0.78	0.21	-0.25	-0.10	4.36	-0.19	+0.01	11.47
-18	Sb	III	+0.90	+0.30	40.36	+0.76	+0.12	46.48	+0.43	-0.42	8.14
-19	Sb	III	+0.72	+0.23	14.49	+0.43	-0.22	11.69	+0.33	-0.32	0.71
-20	Sb	II	+0.41	-0.04	6.98	+0.26	-0.21	0.94	+0.19	-0.27	2.38
-21	Sb	I	-0.04	-0.44	1.40	+0.07	-0.21	3.42	+0.04	-0.21	8.90
-22	Sb	I	-0.68	-0.97	0.15	-0.24	-0.30	4.11	-0.19	-0.20	10.92
-18	Sc	III	+1.25	+0.70	53.73	+1.26	+0.94	9.73	+0.66	-0.26	7.10
-19	Sc	III	+0.98	+0.43	8.58	+0.75	+0.08	9.96	+0.48	-0.34	6.32
-20	Sc	I	+0.73	+0.22	1.72	+0.49	-0.14	3.09	+0.35	-0.30	10.32
-21	Sc	I	+0.39	-0.08	0.32	+0.30	-0.16	3.89	+0.19	-0.27	15.24
-22	Sc	I	-0.15	-0.59	0.48	+0.01	-0.27	10.35	-0.02	-0.27	19.38

^a M_B = absolute B -magnitude.

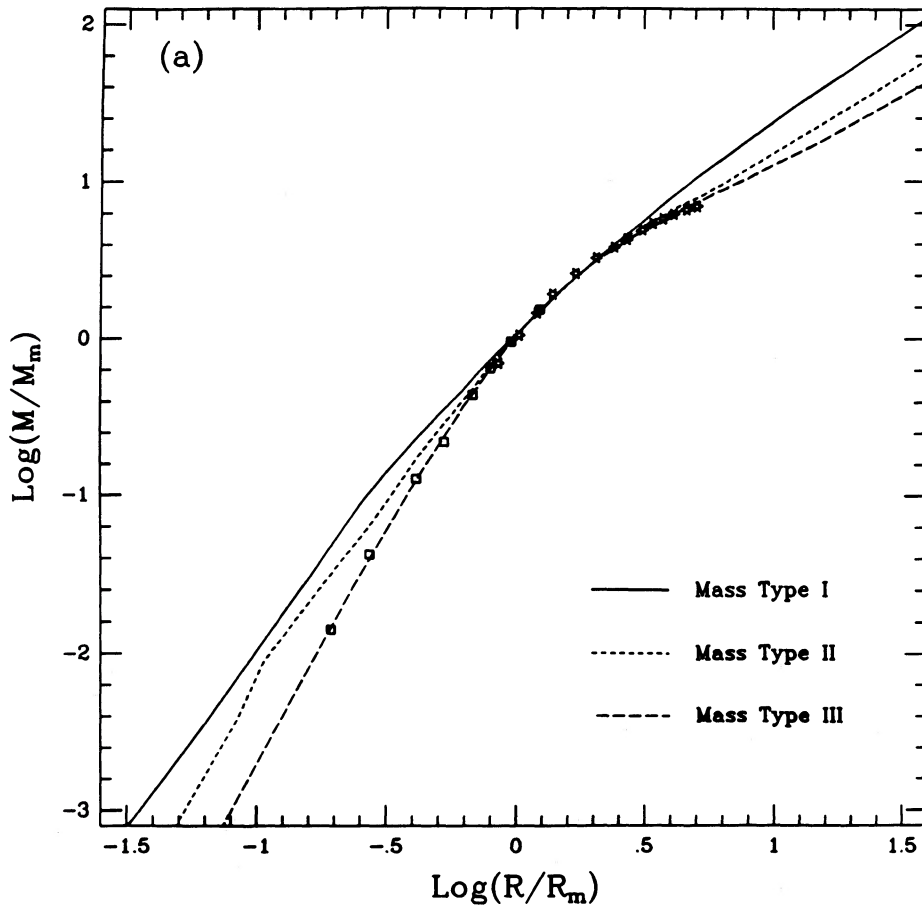


FIG. 1.—(a) Templates for the three mass types, as defined in BR, with two different fits to mass type III. (b) The corresponding rising rotation curve for a fit to the lower portion of mass type III. (c) The corresponding falling rotation curve for a fit to the upper portion of mass type III.

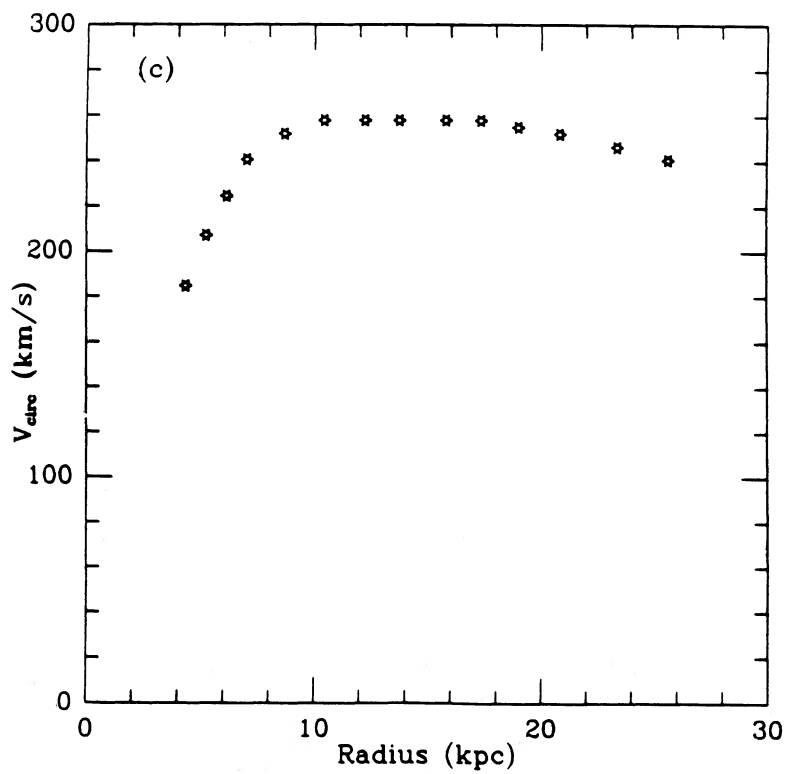
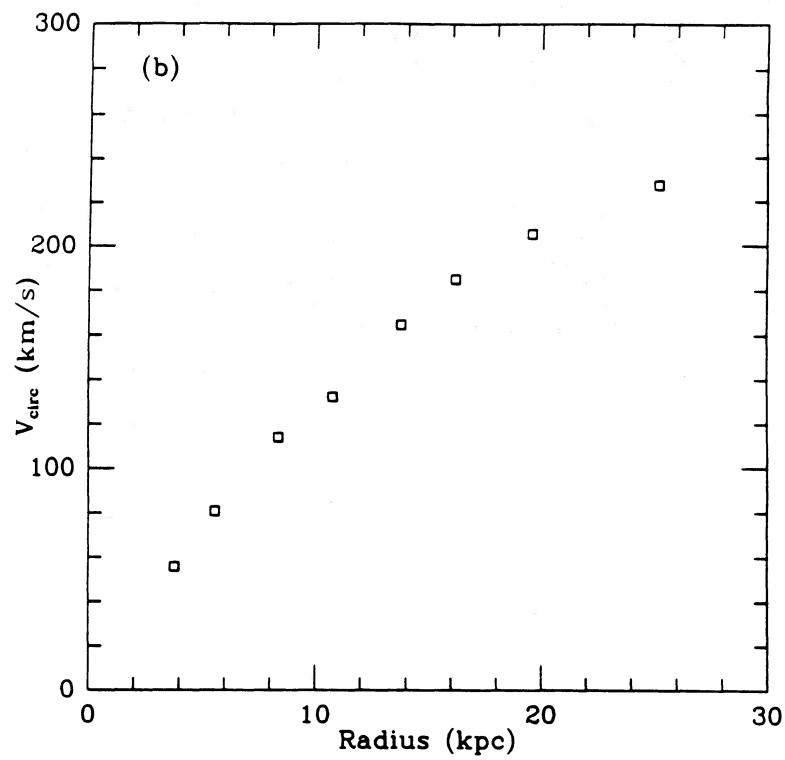


FIG. 1—Continued

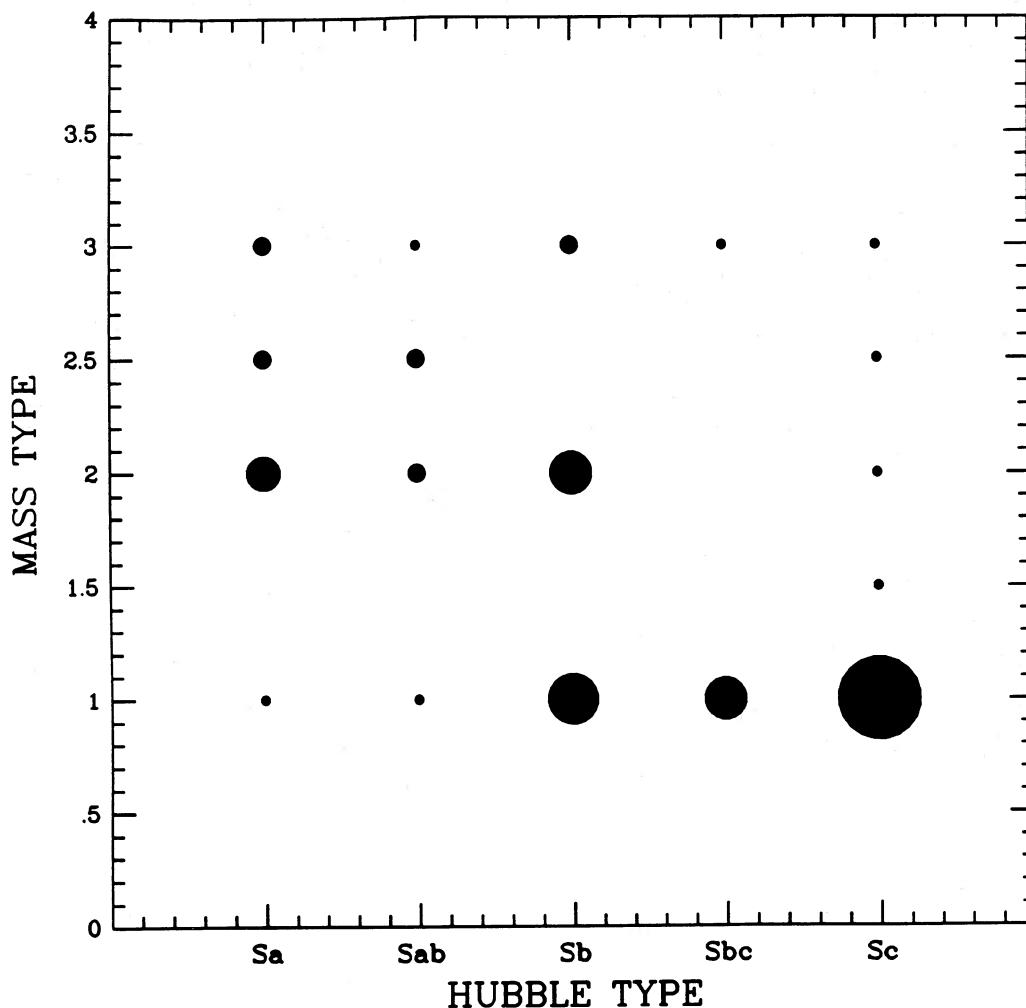


FIG. 2.—Correlation between mass type and Hubble type for the $H\alpha$ -FIELD sample. The diameters of the circles are proportional to the number of data points they represent (i.e., the largest circle has 10 data points associated with it; the smallest represents only one data point). Although the discrete nature of the parameters makes a graphical representation difficult, the correlation coefficient is 0.47, resulting in a probability of 99.9% that mass type and Hubble type are correlated.

Eight cluster spirals have been classified as UNC, primarily because of their small dynamic range. Only three field spirals are unclear. Guhathakurta *et al.* (1988) note that NGC 4222, NGC 4237, NGC 4568, and NGC 4689 were observed with insufficient angular resolution. We classified all of these galaxies as UNC because of insufficient dynamic range, hence they had no effect on our results. We find no significant difference between the cluster and field samples. This may be because inner cluster galaxies, which tend to have a low total H I content, were not well represented in our sample (i.e., there are only five galaxies within 0.8 Mpc of the cluster center). Hence, the sample was made up primarily of galaxies in the outer region of clusters, for which WFR have shown that the rotation curves are similar in nature to those of field galaxies. The Kolmogorov-Smirnov test indicates that the two distributions are indistinguishable.

iii) Discussion

WFR find that the outer gradient in rotation curves correlates well with the distance of the galaxy from the center of the cluster (R_{cluster}), in the sense that galaxies with a negative OG (i.e., falling rotation curve) tend to be found only in the inner

regions of clusters. Since mass types correlate with OG, we might also expect to see this effect in the distribution of mass type with position within the cluster.

Figure 8 shows the distribution of mass types for galaxies in the inner and outer regions of the clusters for the $H\alpha$ -CLUSTER sample. The equivalent for the H I-CLUSTER sample is shown in Figure 9. In both the $H\alpha$ and the H I samples, mass type I galaxies are preferentially found in the outer region of clusters. There is a trend for mass type III to be associated with the inner cluster regions in the $H\alpha$ -CLUSTER sample. This is not evident in the H I-CLUSTER sample. These trends are not as strong as WFR found between OG and R_{cluster} .

In retrospect, it appears that the BRFW result (i.e., fewer mass types I's in clusters) can be understood in terms of the correlation between OG and R_{cluster} discovered by WFR, and between OG and mass types as discussed earlier in this section.

IV. SUMMARY

Recent papers by Burstein and Rubin (1985) and Burstein *et al.* (1986) have been reexamined using both a new objective

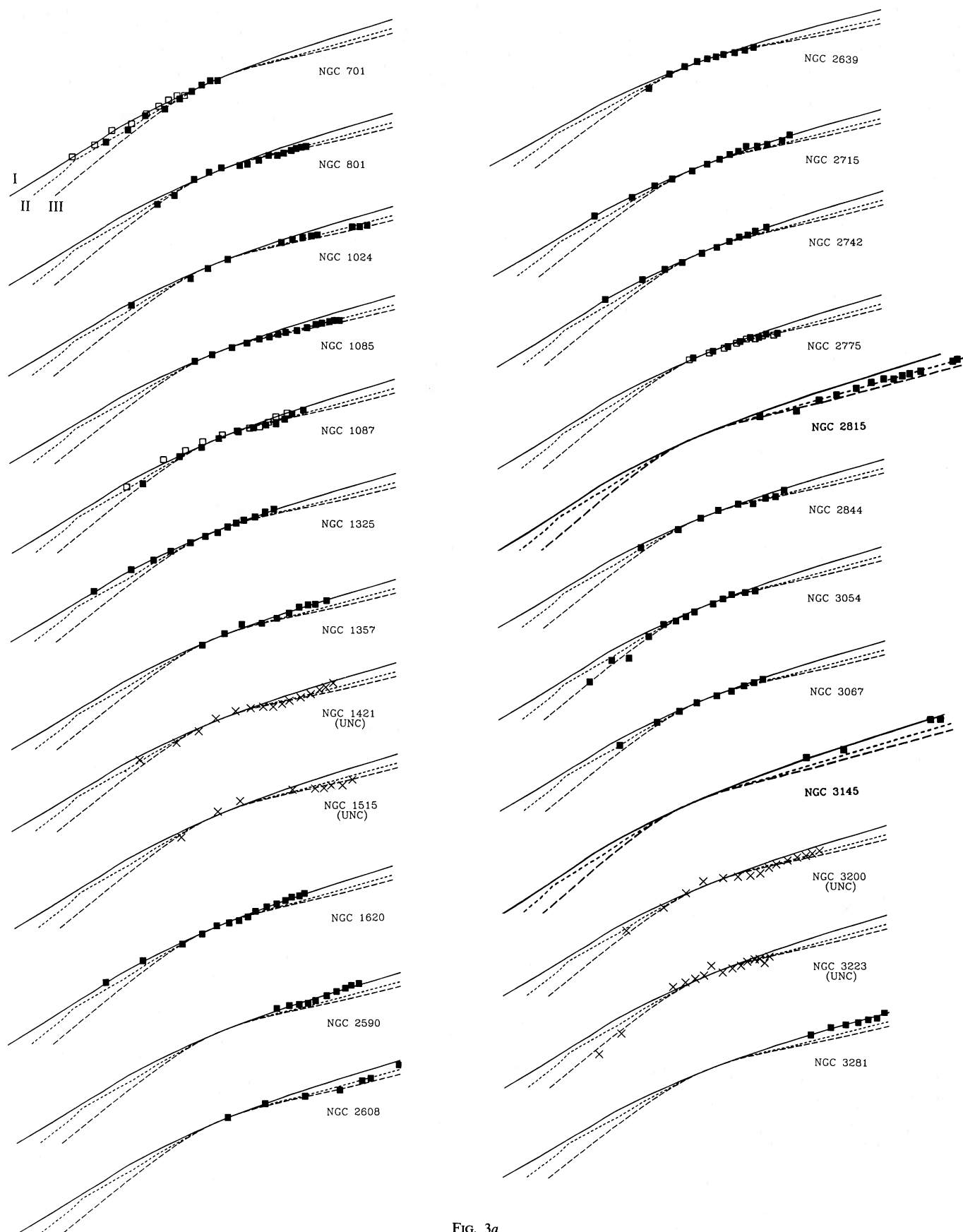


FIG. 3a

FIG. 3.—Best fits to Burstein's mass types for (a, b) $H\alpha$ -FIELD and (c) $H\alpha$ -CLUSTER samples. The same scale is used as in Fig. 1. The best fits are represented by filled squares. Intermediate fits have filled squares for the best fit and open squares for the second-best fit. Unclear fits are represented by crosses.

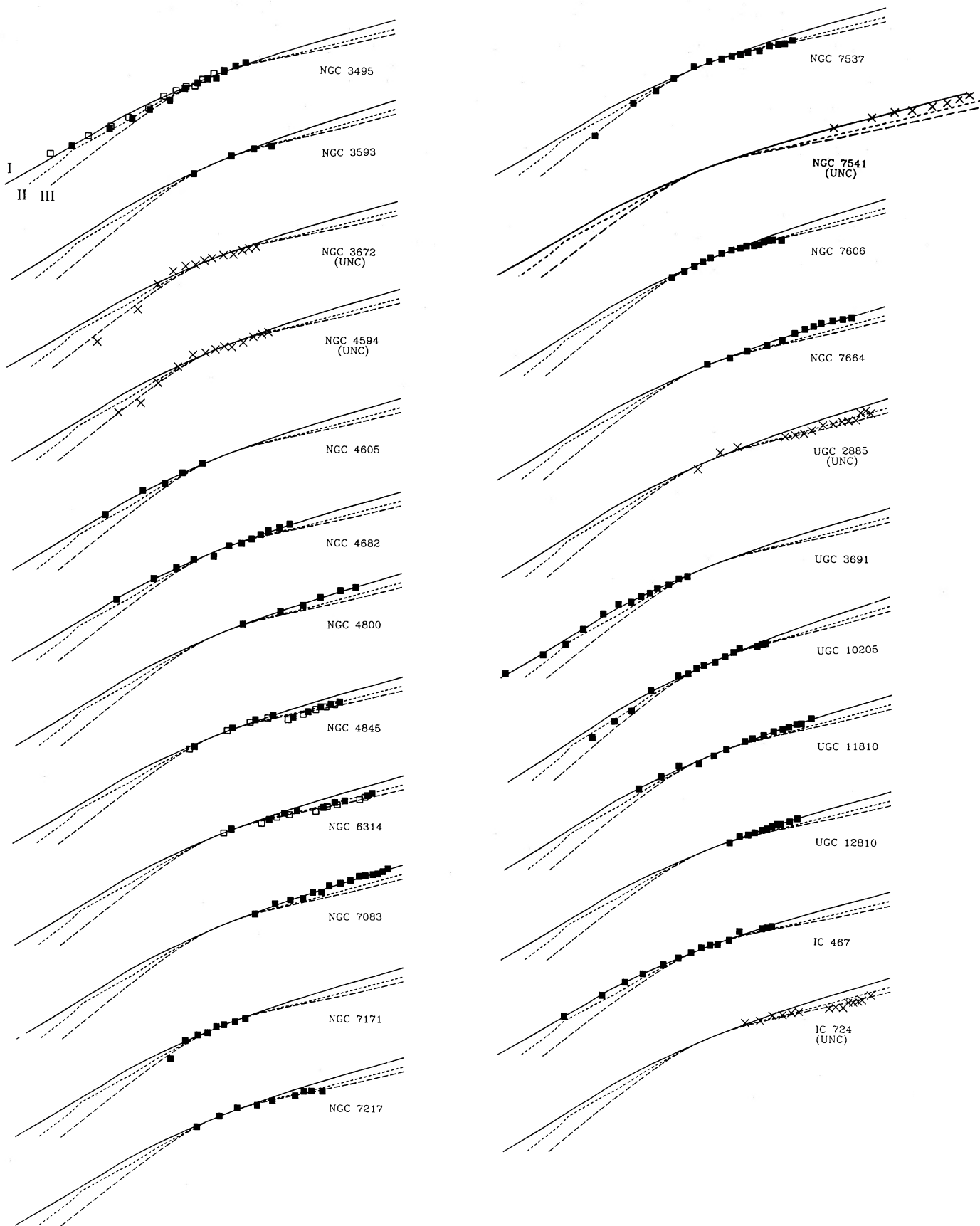


FIG. 3b

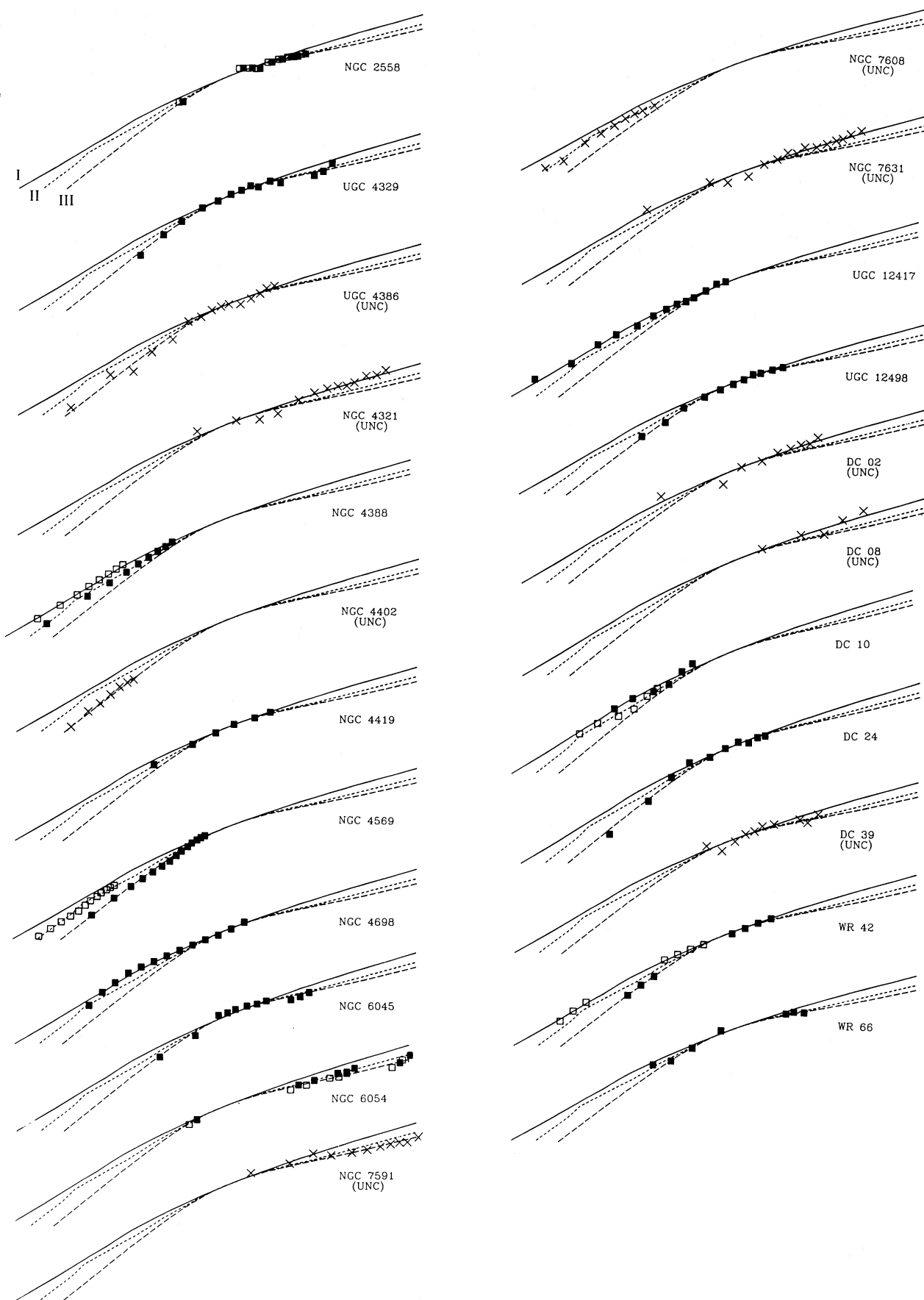


FIG. 3c

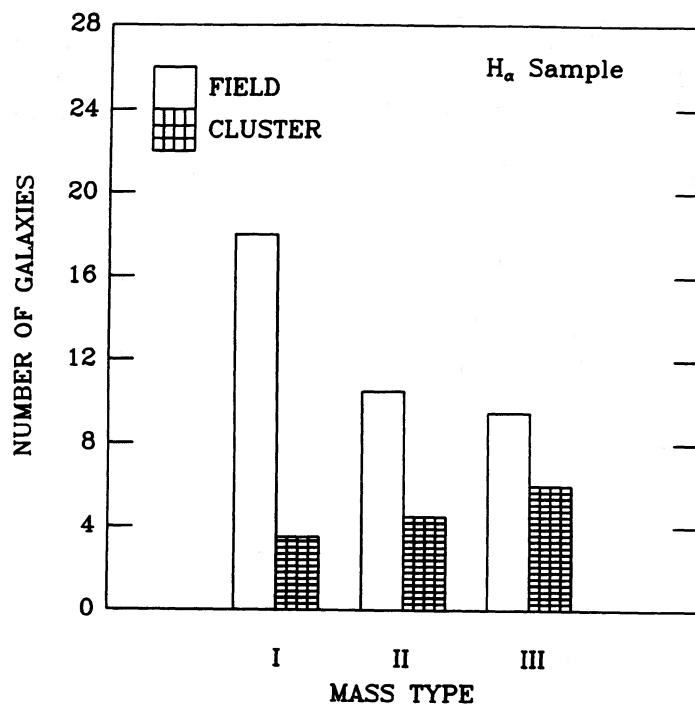


FIG. 4.—Distribution of mass types for the H α sample. A deficiency of mass type I in the cluster sample found by BRFW (see their Fig. 3b) is supported. In the cases for which two mass types have been assigned in Tables 1 and 2, half is represented in each mass type. This also applies to Figs 7–9.

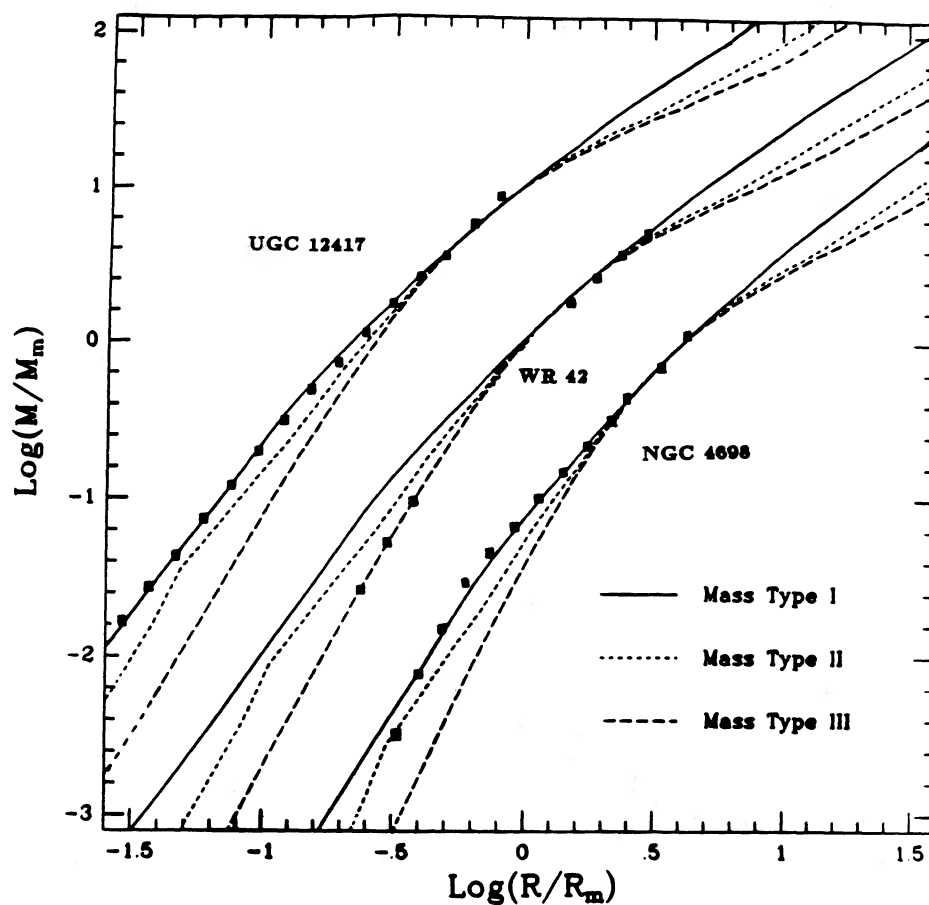


FIG. 5.—Best fits for three cluster galaxies for which BRFW and our study give discrepant results. UGC 12417 (mass type I) has been classified by BRFW as mass type II. WR 42 (mass type I–III) was classified by BRFW as mass type III; however, this does not reflect how poorly the mass type is actually determined in this case. Shown here is the best fit to mass type III. NGC 4698 (mass type I) was also classified as mass type I by BRFW; however, they included it in their field sample. We have included it in our H α -CLUSTER sample. See text for details.

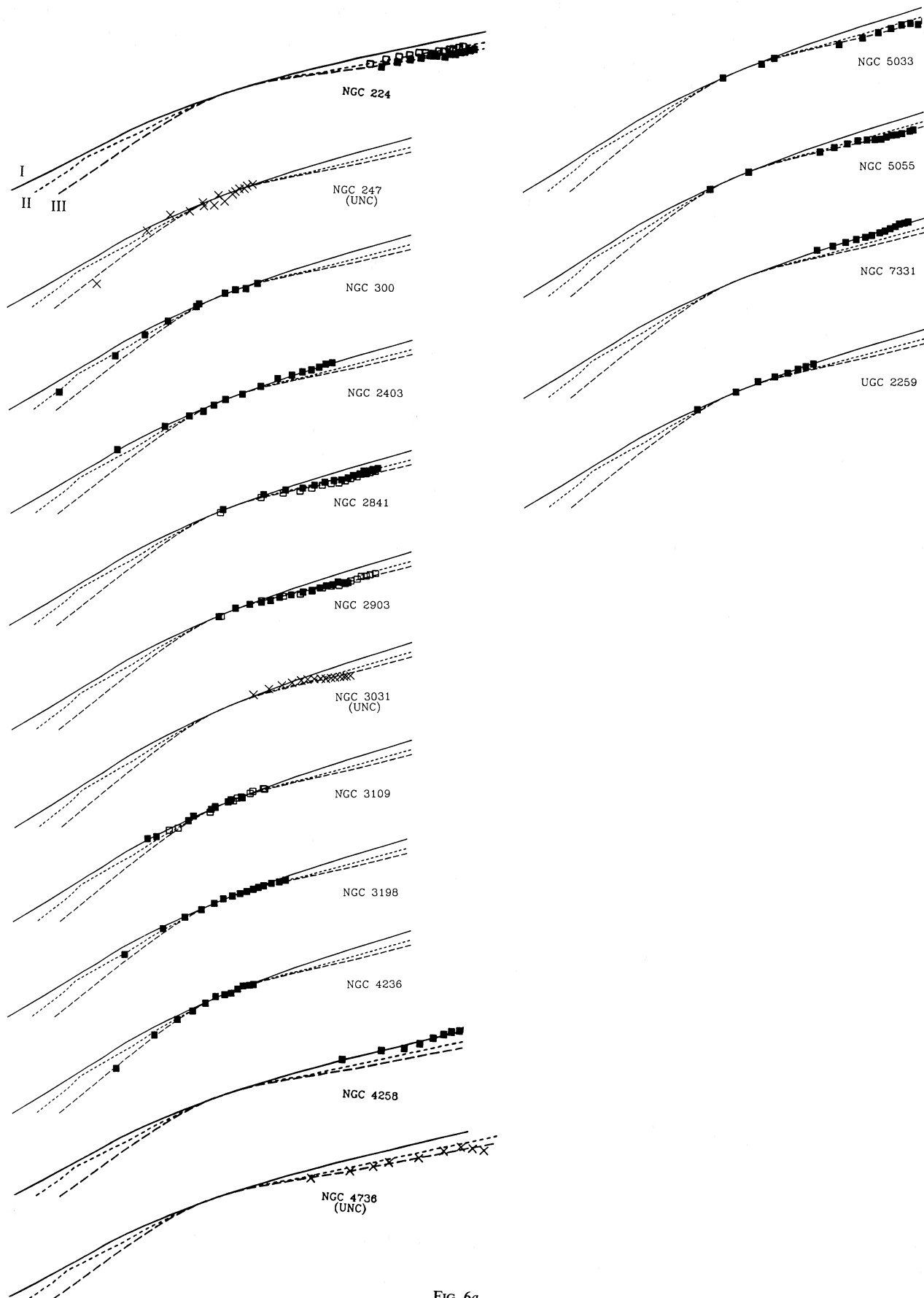


FIG. 6a

FIG. 6.—Best fits to Burstein's mass types for (a) H I-FIELD and (b) H I-CLUSTER samples. The same scale and symbols are used as in Figure 3.

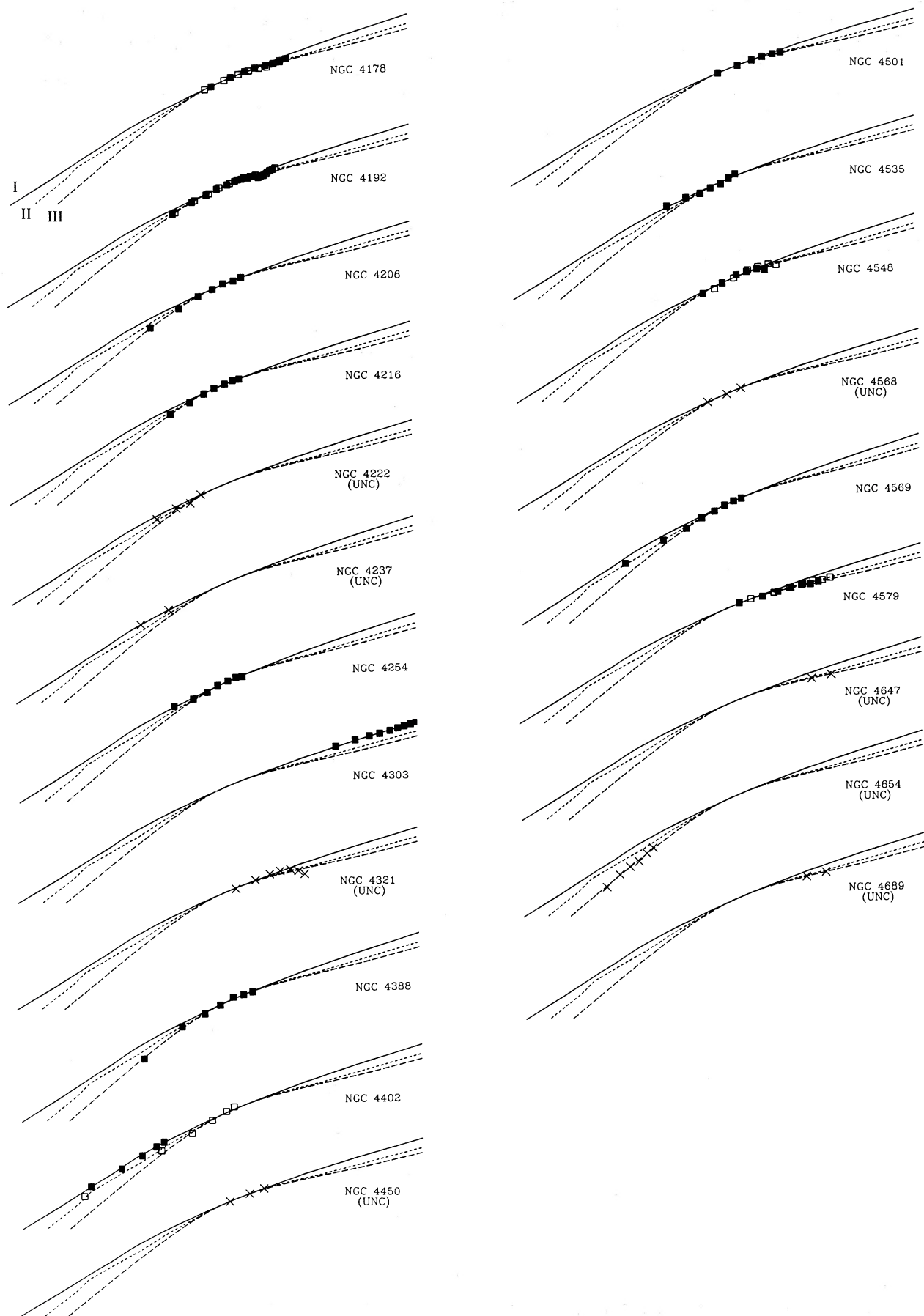


FIG. 6b
671

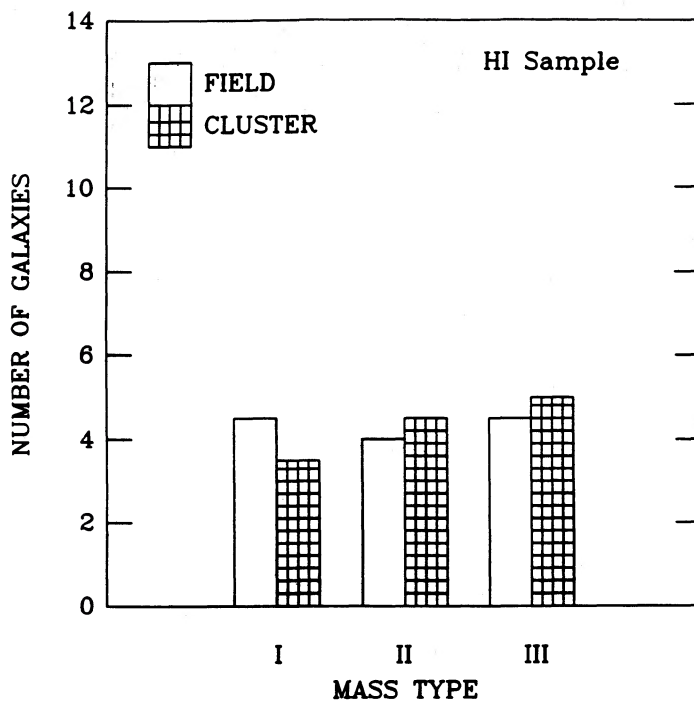


FIG. 7.—Distribution of mass types for the H I sample. The sample is made up primarily of galaxies in the outer region of the Virgo Cluster. This may explain the similarity between the H I-FIELD and H I-CLUSTER samples.

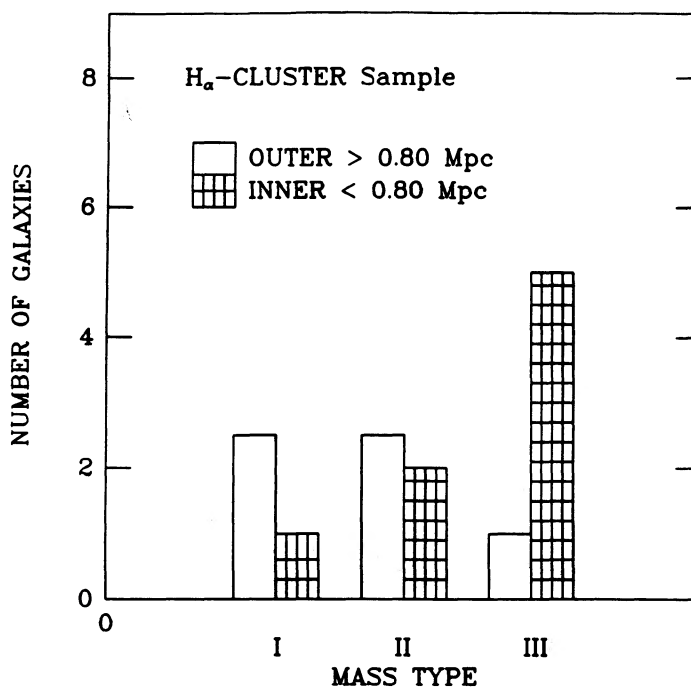


FIG. 8.—Distribution of mass type as a function of position within the cluster for the H α -CLUSTER sample. There is a trend for mass type I to be associated with the outer cluster regions and mass type III with the inner regions.

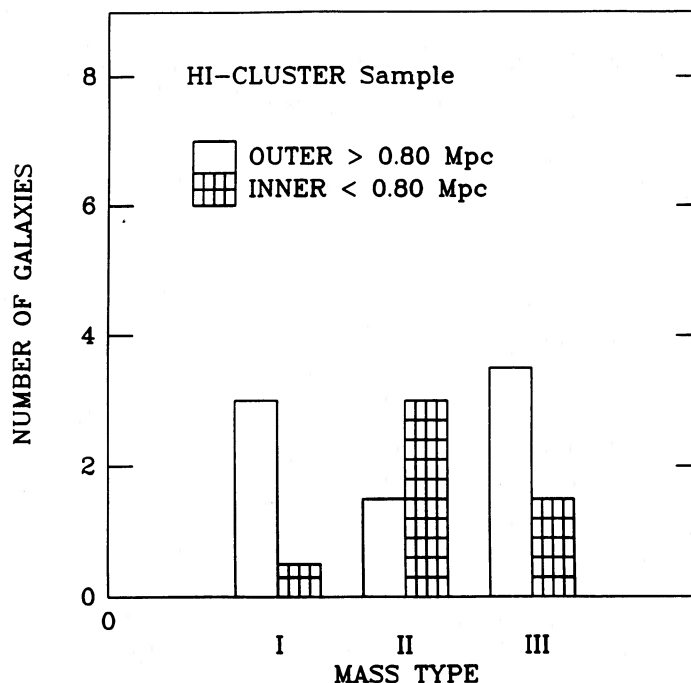


FIG. 9.—Distribution of mass type as a function of position within the cluster for the H I-CLUSTER sample

technique and more recent observational data. In conclusion:

1. The agreement between the mass types determined using our objective χ^2 method and using the earlier fitting technique of BR and BRFW was very good. The agreement for the H α -FIELD sample was better than that for the H α -CLUSTER sample, presumably because the quality of the rotation curves was better.

2. Mass types correlate with many properties of the luminous galaxy. In particular, a least-squares analysis of 49 galaxies reveals a correlation with B -luminosity ($R = 0.22$) and an even stronger correlation with Hubble type ($R = 0.47$) in the sense that Sa galaxies tend to be of mass type II-III and Sc galaxies tend to be of mass type I (this was noted by BR). Analysis of Rubin's synthetic rotation curves confirms that mass types are a function of luminosity; the correlation with Hubble type is not as evident.

3. A comparison between the mass distributions of spiral galaxies in clusters and in the field shows a difference for the H α sample, substantiating the result of BRFW. The lack of a clear correlation in the H I sample is probably due to the absence of many inner cluster galaxies in our sample.

4. A weak correlation of mass type with the position within the cluster is evident, namely, mass type III is associated with the inner regions and mass type I is found only in the outer regions of the cluster. This is similar, but weaker, than the correlation found between the outer gradient and the position of the galaxy within the cluster (R_{cluster}) found by Whitmore, Forbes, and Rubin (1988).

We would like to thank P. Guhathakurta, J. H. van Gorkom, C. G. Kotanyi, and C. Balkowski for allowing us to use their data prior to publication, and D. Burstein for discussions on how he determined his mass types.

REFERENCES

- Athanassoula, S., Bosma, A., and Papaioannou, S. 1987, *Astr. Ap.*, **179**, 23.
 Bevington, P. R. 1969, *Data Reduction and Error Analysis for the Physical Sciences* (New York: McGraw-Hill).
 Burstein, D., and Rubin, V. C. 1985, *Ap. J.*, **297**, 423 (BR).
 Burstein, D., Rubin, V. C., Ford, W. K., and Whitmore, B. C. 1986, *Ap. J. (Letters)*, **305**, L11 (BRFW).
 Chincarini, G., and de Souza, R. 1985, *Astr. Ap.*, **153**, 218.
 de Vaucouleurs, G., de Vaucouleurs, A., and Corwin, H. G. 1976, *Second Reference Catalogue of Bright Galaxies* (Austin: University of Texas Press) (RC2).
 Guhathakurta, P., van Gorkom, J. H., Kotanyi, C. G., and Balkowski, C. 1988, *A. J.*, **96**, 851.
 Kent, S. 1986, *A. J.*, **91**, 1301.
 ———. 1987, *A. J.*, **93**, 816.
 Nilson, P. 1973, *Uppsala General Catalogue of Galaxies* (Uppsala Astr. Obs. Ann., Vol. 6) (UCG).
 Rubin, V. C., Burstein, D., Ford, W. K., and Thonnard, N. 1985, *Ap. J.*, **289**, 81.
 Rubin, V. C., Whitmore, B. C., and Ford, W. K. 1988, *Ap. J.*, **333**, 522.
 Sandage, A., and Tammann, G. A. 1981, *A Revised Shapley-Ames Catalog of Bright Galaxies* (Washington, DC: Carnegie Institution of Washington) (RSA).
 Whitmore, B. C. 1984, *Ap. J.*, **278**, 61.
 Whitmore, B. C., Forbes, D. A., and Rubin, V. C. 1988, *Ap. J.*, **333**, 542 (WFR).

DUNCAN A. FORBES: Institute of Astronomy, University of Cambridge, Cambridge CB3 0HA, United Kingdom

BRADLEY C. WHITMORE: Space Telescope Science Institute, 3700 San Martin Drive, Baltimore, MD 21218